© 2014. Published by The Company of Biologists Ltd | Development (2014) 141, 1324-1331 doi:10.1242/dev.103044

RESEARCH ARTICLE

# Fertilization-induced K63-linked ubiquitylation mediates clearance of maternal membrane proteins

**Miyuki Sato[1,2,*], Ryosuke Konuma[1], Katsuya Sato[1], Kotone Tomura[1] and Ken Sato[1,*]**


## ABSTRACT

In *Caenorhabditis elegans*, fertilization triggers endocytosis and rapid turnover of maternal surface membrane proteins in lysosomes, although the precise mechanism of this inducible endocytosis is unknown. We found that high levels of K63-linked ubiquitin chains transiently accumulated on endosomes upon fertilization. Endocytosis and the endosomal accumulation of ubiquitin were both regulated downstream of the anaphase-promoting complex, which drives the oocyte's meiotic cell cycle after fertilization. The clearance of maternal membrane proteins and the accumulation of K63-linked ubiquitin on endosomes depended on UBC-13 and UEV-1, which function as an E2 complex that specifically mediates chain elongation of K63-linked polyubiquitin. CAV-1-GFP, an endocytic cargo protein, was modified with K63-linked polyubiquitin in a UBC-13/UEV-1-dependent manner. In *ubc-13* or *uev-1* mutants, CAV-1-GFP and other membrane proteins were internalized from the plasma membrane normally after fertilization. However, they were not efficiently targeted to the multivesicular body (MVB) pathway but recycled to the cell surface. Our results suggest that UBC-13-dependent K63-linked ubiquitylation is required for proper MVB sorting rather than for internalization. These results also demonstrate a developmentally controlled function of K63-linked ubiquitylation.


**KEY WORDS: Endocytosis, Oocyte-to-zygote transition, K63-linked ubiquitin chains, Ubc13, Multivesicular body (MVB) pathway**

## INTRODUCTION

The oocyte-to-zygote (embryo) transition is the process by which oocytes transform to totipotent zygotes. It is one of the most dramatic examples of cellular remodeling in animals, and the active degradation of pre-existing materials is an essential part of this transition (Stitzel and Seydoux, 2007; Sato and Sato, 2013). The importance of the ubiquitin-proteasome system in this process has been established. Some oocyte meiotic proteins are harmful for mitosis, and they must be degraded by the proteasome for normal mitotic cell division (Bowerman and Kurz, 2006). The proteasome also mediates the degradation of germ cell-specific proteins in somatic lineages, starting as early as the two-cell-stage embryo (Spike and Strome, 2003). Additionally, autophagy is induced upon sperm entry to deliver paternal (allogeneic) organelles, including mitochondria and membranous organelles (MOs), to the lysosomes for degradation (allophagy) (Sato and Sato, 2011; Al Rawi et al., 2011). We have previously shown that endocytosis is highly upregulated during this period, leading to the rapid turnover of maternal plasma membrane (PM) proteins in *Caenorhabditis elegans* embryos (Sato et al., 2006; Sato and Sato, 2013). This was first visualized by using CAV-1 (a worm caveolin homolog) fused with GFP (CAV-1-GFP) (Sato et al., 2006). In oocytes, CAV-1-GFP accumulates on cortical granules (CGs). Shortly after fertilization, CAV-1-GFP is delivered to the PM by CG exocytosis. CAV-1-GFP targeted to the PM is then quickly endocytosed and degraded in lysosomes before the first mitotic division. In addition to CAV-1-GFP, several maternal membrane proteins, including the yolk receptor RME-2 and the putative sperm receptor EGG-1, are downregulated with a similar time course (Kadandale et al., 2005; Audhya et al., 2007; Balklava et al., 2007). The degradation of maternal membrane proteins is a selective process because GFP fusions of SNB-1 (a synaptobrevin homolog) and SYN-4 (a syntaxin1 homolog), which also localize to the PM of fertilized embryos, are not degraded (Sato et al., 2008).

Ubiquitylation is a post-translational modification involved in proteasomal degradation and various other cellular processes, including endocytosis. Proteins can be modified with a single ubiquitin molecule or a chain of ubiquitins, which are linked through one of the seven lysine residues or the N-terminus of ubiquitin. The diverse types of ubiquitin modifications are thought to have specific functions. Among them, K63-linked polyubiquitylation is involved in DNA repair, various signaling pathways and the endocytosis of membrane proteins (Pickart and Fushman, 2004; Kerscher et al., 2006; Mukhopadhyay and Riezman, 2007). K63- and K48-linked ubiquitylation are induced on paternal MOs in worm embryos before allophagy (Sato and Sato, 2011; Al Rawi et al., 2011). Ubiquitylation is mediated by the sequential action of ubiquitin-activating enzymes (Uba or E1), ubiquitin-conjugating enzymes (Ubc or E2), and ubiquitin ligases (E3) (Kerscher et al., 2006). Substrate recognition largely depends on E3 enzymes, whereas E2 enzymes determine the topology of the ubiquitin modification. Some E2 enzymes mediate the attachment of the first ubiquitin to the lysine residues of the target protein (chain initiation), and others mediate further chain elongation (Ye and Rape, 2009). To date, Ubc13 is the only E2 shown to specifically mediate the elongation of K63-linked polyubiquitin chains. Ubc13 functions in a dimeric complex with the non-catalytic E2 variant Uev1A or Mms2 (Hofmann and Pickart, 1999; Deng et al., 2000; Eddins et al., 2006). In mice, knockout of Ubc13 results in early embryonic lethality, and conditional knockout in myeloid cells or heterozygosity produces defects in the immune response and hematopoiesis (Yamamoto et al., 2006; Fukushima et al., 2007; Wu et al., 2009). In *C. elegans*, UEV-1 is involved in the trafficking of glutamate receptor GLR-1 in neurons (Kramer et al., 2010). However, our understanding of the physiological roles of K63-linked ubiquitylation in animals is still limited.

Ubiquitylation can regulate different steps of endocytosis (Mukhopadhyay and Riezman, 2007; Traub and Lukacs, 2007; Lauwers et al., 2010). Monoubiquitylation (single or multiple) or K63-linked polyubiquitylation of cargo molecules has been reported

[1]Laboratory of Molecular Traffic, Institute for Molecular and Cellular Regulation, Gunma University, Maebashi, Gunma 371-8512, Japan. [2]Laboratory of Molecular Membrane Biology, Institute for Molecular and Cellular Regulation, Gunma University, Maebashi, Gunma 371-8512, Japan.

*Authors for correspondence (m-sato@gunma-u.ac.jp; sato-ken@gunma-u.ac.jp)

**Received 26 August 2013; Accepted 6 January 2014**

Development (2014) doi:10.1242/dev.103044

to be required for internalization from the PM (Mukhopadhyay and Riezman, 2007; Traub and Lukacs, 2007). Ubiquitylation is also involved in subsequent cargo sorting at late endosomes, alternatively called multivesicular bodies (MVBs). Membrane proteins destined for degradation are sorted into intraluminal vesicles (ILVs) at the endosomal membrane; the resulting MVBs then fuse with lysosomes for the degradation of their contents. ILV formation and cargo sorting are mediated by the endosomal sorting complex required for transport (ESCRT) machinery (Raiborg and Stenmark, 2009). Previous studies indicate that K63-linked polyubiquitylation of cargo proteins specifically functions as an ESCRT-dependent sorting signal to ILVs rather than as an internalization signal (Huang et al., 2006; Barriere et al., 2007; Lauwers et al., 2010; Erpapazoglou et al., 2012), although other reports suggest that multiple or even single monoubiquitylation is sufficient for MVB sorting (Stringer and Piper, 2011). Thus, the exact role of K63-linked ubiquitylation in endocytic processes remains controversial.

In this study, we show that K63-linked ubiquitylation is strongly induced upon fertilization. K63-linked ubiquitin chains transiently accumulate on the endosomes of one-cell-stage embryos. This process is regulated in *C. elegans* by UBC-13 and UEV-1 and by cell cycle progression after fertilization. In *ubc-13* and *uev-1* mutants, maternal membrane proteins are internalized from the PM but are inefficiently targeted to lysosomes, suggesting that K63-linked ubiquitylation is required for efficient MVB sorting rather than for internalization from the PM. These results also demonstrate a new physiological function of K63-linked ubiquitylation during animal development.

## RESULTS

### Fertilization induces transient accumulation of K63-linked ubiquitin chains on endosomes

Degradative endocytosis is highly upregulated in the one-cell-stage embryo (Sato et al., 2006). Because ubiquitylation was reported to be involved in endocytic uptake and sorting into the MVB pathway, we hypothesized that the intracellular ubiquitylation state is dynamically regulated in early embryos. To test this, oocytes and embryos were stained with an anti-ubiquitin antibody that recognizes ubiquitin conjugated to proteins but not free ubiquitin (FK2). In *C. elegans*, oocytes temporarily arrest in prophase of meiosis I. After fertilization, the oocytes complete meiosis I and II, and the first mitotic division takes place ~65 minutes after fertilization (supplementary material Fig. S1A) (McCarter et al., 1999). CAV-1-GFP on CGs is exocytosed during anaphase I and then rapidly internalized in meiosis II (Sato et al., 2006). In growing oocytes, weak ubiquitin signals were observed in nuclei and several small puncta (supplementary material Fig. S1B). During ovulation, oocytes showed transient weak staining for ubiquitin on small cortical puncta, presumably cortical endosomes (supplementary material Fig. S1B, −1 oocyte). By contrast, in the early one-cell-stage embryo just after fertilization (metaphase I), strong accumulation of ubiquitin was first detected on sperm-derived MOs, as reported previously (Fig. 1A) (Sato and Sato, 2011; Al Rawi et al., 2011). MOs are specialized post-Golgi organelles that are destined for autophagic degradation in embryos (L'Hernault, 2006; Sato and Sato, 2011; Al Rawi et al., 2011). As the cell cycle progressed to meiosis II, a dramatic increase in the ubiquitin signal on cortical puncta and ring-shaped structures was observed in addition to the signal on MOs (Fig. 1B,B′). This ubiquitin accumulation was transient, and most of the signals on cortical puncta disappeared by the two-cell stage (Fig. 1C). We also examined the linkage specificity of the ubiquitylation by using anti-K48- and anti-K63-linked polyubiquitin antibodies (Apu2 and Apu3, respectively) (Newton et al., 2008). Paternal MOs were recognized by both antibodies (Fig. 1A,D), as previously reported (Sato and Sato, 2011; Al Rawi et al., 2011). By contrast, the cortical puncta that appeared during meiosis II were stained only with the anti-K63-specific polyubiquitin antibody (Fig. 1B′,E′). FK2 and Apu2 also stained the cleavage furrow, but Apu3 did not (Fig. 1F).

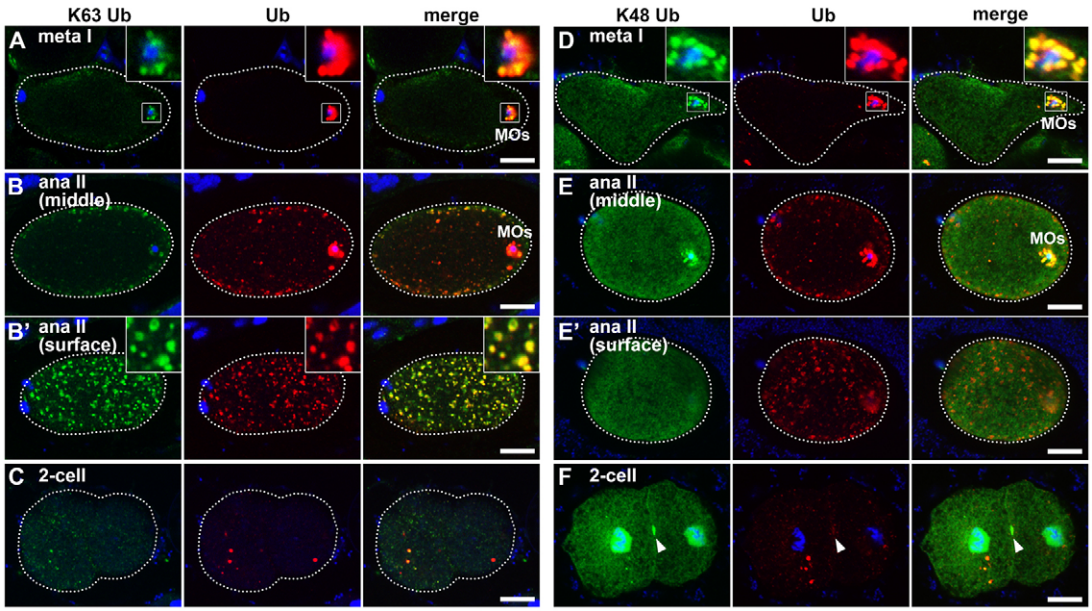


**Fig. 1. Dynamic regulation of the cellular ubiquitylation state in early embryos.** Wild-type N2 embryos were dissected from adult hermaphrodites and stained with an anti-ubiquitin antibody (FK2; red) and an anti-K63-linked ubiquitin (Apu3; A-C) or anti-K48-linked ubiquitin (Apu2; D-F) antibody (green). Blue shows DAPI staining. In all images, dotted lines indicate the outline of the embryos. The insets show enlarged images (×3). Note that the anti-K63-linked ubiquitin antibody stained MOs and cortical endosomes at comparable levels, whereas the anti-ubiquitin antibody stained MOs more strongly. The punctate ubiquitin staining in the two-cell-stage embryos are MOs (C,F). The anti-K48-linked ubiquitin antibody stained the cleavage furrow (F, arrowheads). Scale bars: 10 µm.

Development (2014) doi:10.1242/dev.103044

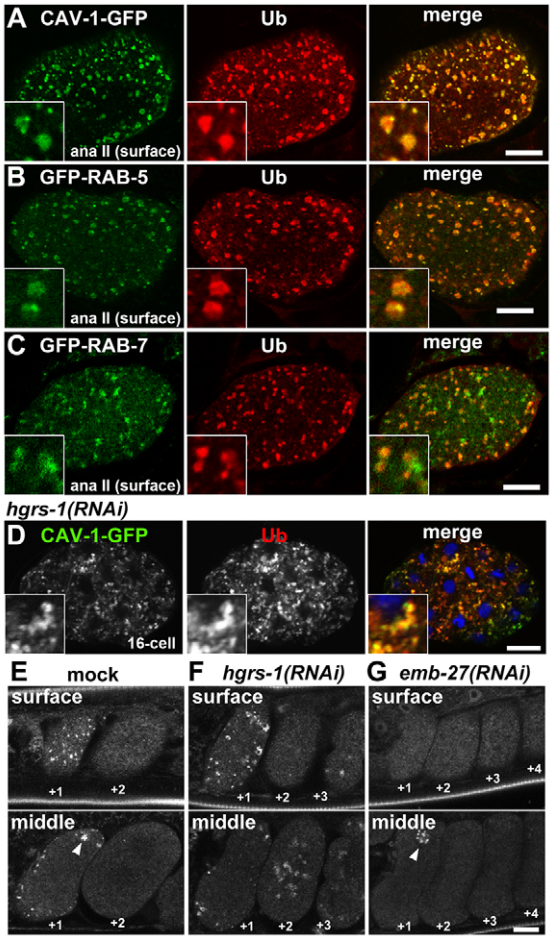


**Fig. 2. Ubiquitin accumulates on endosomes in one-cell-stage embryos.** (A-C) Embryos expressing CAV-1-GFP (A), GFP-RAB-5 (B) or GFP-RAB-7 (C) were stained with an anti-ubiquitin antibody. Images of the surface of embryos during anaphase in meiosis II are shown. The insets show enlarged images (×3). (D) Knockdown of *hgrs-1* causes ubiquitin and CAV-1-GFP to accumulate in aberrant endosomes. Worms expressing CAV-1-GFP were treated with *hgrs-1* RNAi. A 16-cell-stage embryo stained with an anti-ubiquitin antibody (red) and DAPI (blue) is shown. The insets show enlarged images (×3). (E-G) The dynamic behavior of GFP-Ub in live embryos was observed in intact animals. The embryos are numbered according to their position from the spermatheca, and the +1 embryos are the most recently fertilized. The arrowheads indicate signals on paternal MOs. (E) mock; (F) *hgrs-1(RNAi)*; (G) *emb-27(RNAi)*. Scale bars: 10 µm.

Colocalization of ubiquitin staining with GFP-RAB-5, a marker of early endosomes, and with endocytosed CAV-1-GFP (Fig. 2A,B) confirmed that the cortical structures were endosomes. The ubiquitin-positive endosomes were also positive for GFP-RAB-7, although the GFP-RAB-7 and ubiquitin signals showed a mosaic pattern on the same structures (Fig. 2C). Apu2 and Apu3 antibodies were pre-absorbed with purified polyubiquitin to verify their linkage-specificity (Newton et al., 2008). Apu2 staining was specifically inhibited by pre-absorption with K48-linked polyubiquitin (supplementary material Fig. S2A-F). Apu3 staining of endosomes and MOs was completely abolished by preincubation with K63-linked polyubiquitin; excess K48-linked polyubiquitin partially competed with Apu3 (supplementary material Fig. S2G-N). These results suggest that Apu3 has a strong affinity for K63-linked polyubiquitin and retains a weak reactivity toward K48-linked polyubiquitin in certain conditions. However, staining of endosomes specifically with Apu3 but not with Apu2 in our conditions strongly suggests that K63-linked ubiquitin accumulates on endosomes. A different anti-K63-linked polyubiquitin antibody (D7A11) also stained CAV-1-GFP-positive endosomes (supplementary material Fig. S3A). Taken together, these results demonstrate that fertilization triggers massive and temporal accumulation of K63-linked polyubiquitin on endosomes. We do not exclude the possibility that other types of ubiquitin chains also exist on endosomes and MOs. In embryos at late anaphase I, in which endocytic cargo still localized mainly on the PM, staining with anti-ubiquitin (FK2) and anti-K63-linked ubiquitin (Apu3) antibodies was detected on the cell surface (supplementary material Fig. S3B,C). When cargo accumulated on endosomes in subsequent meiosis II, the ubiquitin staining also accumulated on endosomes and appeared to increase in total intensity. These observations suggest that ubiquitylation starts at the cell surface and progresses to the endosomes during endocytic trafficking.

The degradation of internalized CAV-1-GFP is blocked by knockdown of ESCRT subunit genes such as *hgrs-1*, a worm Hrs/Vps27 homolog in the ESCRT-0 complex (Sato et al., 2006; Raiborg and Stenmark, 2009). When we knocked down *hgrs-1*, ubiquitin and endocytosed CAV-1-GFP accumulated on abnormally aggregated endosomes in one-cell-stage embryos and in later-stage embryos (Fig. 2D; data not shown). Thus, the degradation of CAV-1-GFP and the clearance of ubiquitin from endosomes depend on a functional MVB pathway. The dynamic nature of the ubiquitylation was confirmed using worms that express GFP-tagged ubiquitin (GFP-Ub) in the germline. GFP-Ub transiently accumulated on cortical puncta and MOs in one-cell-stage embryos (Fig. 2E). Knockdown of *hgrs-1* resulted in the abnormal accumulation of GFP-Ub on endosomes in later-stage embryos (Fig. 2F).

We also observed changes in the morphology of the endosomes after fertilization. In growing oocytes, GFP-RAB-5 and mRFP-RAB-7 localized on small cortical puncta; their localization only partially overlapped (supplementary material Fig. S4A,A′). After fertilization, the size of the endosomes increased, and GFP-RAB-5 and mRFP-RAB-7 localized on the same enlarged endosomes, although in a mosaic pattern on the membrane (supplementary material Fig. S4B,B′).

### CAV-1-GFP is ubiquitylated after fertilization

We investigated whether endocytic cargo molecules are directly ubiquitylated after fertilization. First, the mobility of CAV-1-GFP molecules was examined by immunoblotting. In lysates of whole wild-type adults, CAV-1-GFP was detected predominantly as bands of ~63 kDa (Fig. 3A, upper panel). Knockdown of *rab-5* strongly blocked degradation of CAV-1-GFP in embryos, and CAV-1-GFP accumulated in small vesicles (Sato et al., 2006). With RNAi of *rab-5*, the ~63 kDa bands and a high molecular mass species of CAV-1-GFP increased slightly. Because a large amount of CAV-1-GFP accumulates in developing oocytes, most CAV-1-GFP in total worm lysates is thought to be protein derived from oocytes. To detect CAV-1-GFP in embryos specifically, we collected early embryos from gravid adults (one-cell stage to ~100-cell stage). In wild-type embryos, a small amount of CAV-1-GFP was detected, confirming the rapid degradation of CAV-1-GFP (Fig. 3A, lower panel, lane 2). When the endocytic flow was blocked by *rab-5* RNAi, a smear of high-molecular mass species was present on immunoblots of embryo lysates, indicating accumulation of the protein (lane 3). Because CAV-1-GFP contains 34 lysine residues in its cytosolic region, it could be ubiquitylated at multiple sites. In fact, a recent study using mass spectrometry suggested that at least two lysine

Development (2014) doi:10.1242/dev.103044

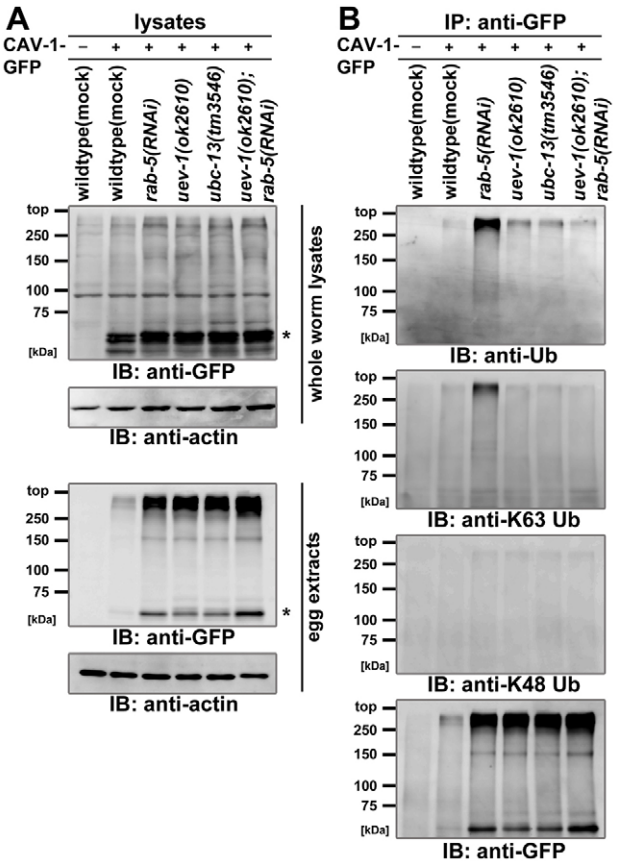


**Fig. 3. CAV-1-GFP is ubiquitylated in embryos.** (A) Whole-worm lysates of mature adults (40 worms; upper panel) or total embryo lysates (10 µg; lower panel) were prepared from the indicated strains and examined by immunoblotting using anti-GFP and anti-actin antibodies. Asterisks indicate CAV-1-GFP that is not ubiquitylated. (B) CAV-1-GFP was immunoprecipitated from total embryo lysates of the indicated strains (70 µg) and probed with an anti-ubiquitin, anti-K63-linked ubiquitin, anti-K48-linked ubiquitin or anti-GFP antibody. The same total embryo lysates were used for immunoblotting (A, lower panel) and immunoprecipitation (B).

residues in GFP-CAV-1 are ubiquitylated in embryos (Mayers et al., 2013). To confirm that the smeared bands corresponded to the ubiquitylated form, CAV-1-GFP was immunoprecipitated from embryo lysates and probed with an anti-ubiquitin antibody (Fig. 3B, upper panel). The anti-ubiquitin antibody recognized the smeared bands from *rab-5(RNAi)* embryos. These species were also recognized by the anti-K63-linked polyubiquitin antibody, but minimally by the anti-K48-linked polyubiquitin antibody, showing that CAV-1-GFP is modified with K63-linked polyubiquitin chains (Fig. 3B, middle panels). The observation that ubiquitylated cargo accumulates after *rab-5* RNAi suggests that ubiquitylation occurs before cargo reaches the early endosomes. This is consistent with morphological observations that ubiquitylation starts at the PM. The results also suggest that CAV-1-GFP is not ubiquitylated in oocytes.

### Endocytosis in fertilized embryos is regulated downstream of the meiotic cell cycle

CAV-1-GFP is targeted to the PM by CG exocytosis and then endocytosed after fertilization (Sato et al., 2006). To monitor endocytosis in fertilized embryos, we looked for other cargo proteins with simpler behavior. We found that chitin synthase CHS-1 is also downregulated by endocytosis in early embryos. CHS-1 is a multispan membrane protein that localizes to the oocyte PM and mediates the synthesis of the chitin layer of the eggshell upon fertilization (Johnston et al., 2010). CHS-1 is also an important regulator of MBK-2, a master kinase that controls the oocyte-to-zygote transition in *C. elegans* (Maruyama et al., 2007; Stitzel et al., 2007; Johnston and Dennis, 2012). As reported previously, GFP-tagged CHS-1 (GFP-CHS-1) localized to the PM in oocytes and very early embryos but relocalized to cortical punctate structures during meiosis II (Fig. 4A,B) (Maruyama et al., 2007). Most of the GFP signal disappeared by the two-cell stage, which is very similar to the behavior of CAV-1-GFP in embryos. Knockdown of *rab-5* inhibited the degradation of GFP-CHS-1, and GFP-CHS-1 localized on small vesicles dispersed in the cytoplasm (Fig. 4C). Furthermore, when the MVB pathway was blocked by *hgrs-1* RNAi, GFP-CHS-1 accumulated on enlarged vesicles (Fig. 4D). These results demonstrate that GFP-CHS-1 is endocytosed and downregulated through the MVB pathway, similar to CAV-1-GFP. CG exocytosis is tightly linked to the onset of anaphase in meiosis I and is blocked when the metaphase-to-anaphase transition is inhibited by knockdown of anaphase promoting complex (APC) subunits such as *emb-27* (Sato et al., 2006). We tested whether the induction of endocytosis also depends on the metaphase-to-anaphase transition by monitoring GFP-CHS-1. Interestingly, the internalization of GFP-CHS-1 from the PM was also strongly blocked by *emb-27* RNAi, suggesting that the induction of endocytosis in fertilized embryos is regulated downstream of the meiotic cell cycle (Fig. 4E). The transient accumulation of GFP-Ub on cortical endosomes was also inhibited by *emb-27* RNAi (Fig. 2G). In contrast to endosomal ubiquitylation, the ubiquitylation on paternal MOs was not inhibited by *emb-27* RNAi (Fig. 2G, arrowhead).

### Sorting of maternal membrane proteins to the MVB pathway is defective in *uev-1* and *ubc-13* mutants

To identify factors that are involved in the ubiquitylation and degradation of maternal membrane proteins, we screened worm E2 genes by RNAi-mediated knockdown. RNAi of *ubc-13* or *uev-1* significantly inhibited the degradation of CAV-1-GFP in embryos (supplementary material Fig. S5A). In these mutants, CAV-1-GFP remained on the PM and endosome-like vesicles in later-stage embryos. Ubc13 forms a complex with E2 variants such as Uev1A and Mms2 and specifically functions in the elongation of K63-linked polyubiquitin chains (Eddins et al., 2006). A similar defect in CAV-1-GFP degradation was observed in *ubc-13(tm3546)* and *uev-1(ok2610)* mutants (Fig. 5A) (Kramer et al., 2010). CG localization of CAV-1-GFP in oocytes and CG exocytosis were normal in both mutants (supplementary material Fig. S5A). Growing oocytes accumulate a large amount of yolk by receptor-mediated endocytosis (Grant and Hirsh, 1999). Neither *ubc-13(RNAi)* nor *uev-1(RNAi)* mutants showed defects in yolk uptake, suggesting that the endocytosis and recycling of the yolk receptor in oocytes were not affected (supplementary material Fig. S5B). The degradation of OMA-1-GFP, which is proteasome dependent, was also normal in *ubc-13(RNAi)* and *uev-1(RNAi)* embryos (supplementary material Fig. S5D) (Spike and Strome, 2003). As reported previously, *ubc-13(tm3546)* and *uev-1(ok2610)* mutants were viable at 20°C (Kramer et al., 2010). However, they showed partial embryonic lethality at 25°C (61% and 68% lethality for *ubc-13(tm3546)* and *uev-1(ok2610)*, respectively; $n>500$). The simultaneous deletion of *ubc-13* and *uev-1* produced a phenotype nearly identical to the phenotype of each single mutant with respect to CAV-1-GFP accumulation in embryos and viability, supporting the possibility that UBC-13 and UEV-1 function together.

Development (2014) doi:10.1242/dev.103044

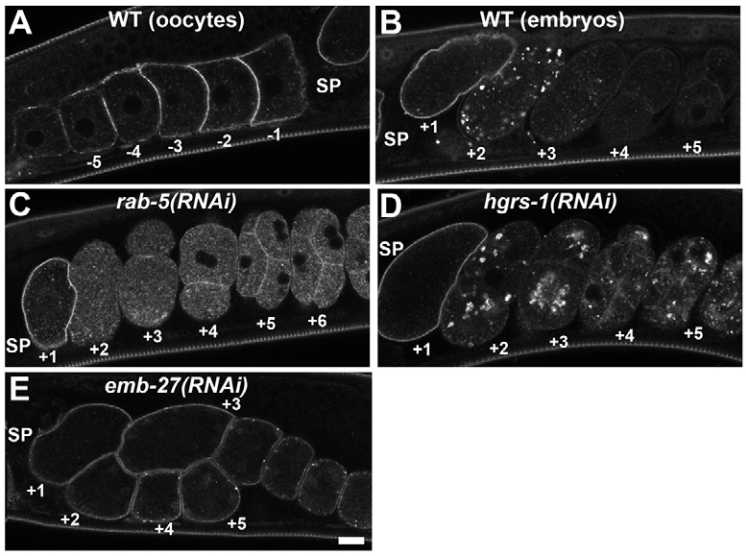


**Fig. 4. Endocytosis of GFP-CHS-1 is regulated downstream of the APC pathway.** (A-E) Oocytes (A) or embryos (B-E) of animals expressing GFP-CHS-1 are shown. (A,B) mock; (C) *rab-5(RNAi)*; (D) *hgrs-1(RNAi)*; (E) *emb-27(RNAi)*. Oocytes and embryos are numbered according to their position from the spermatheca (SP). Scale bar: 10 µm.

The degradation of GFP-CHS-1, GFP-RME-2 and endogenous RME-2 was also inhibited by *ubc-13(tm3546)* and *uev-1(ok2610)* mutations (Fig. 5C; supplementary material Fig. S5C; data not shown). Importantly, even in these mutants, most GFP-CHS-1 was internalized, and it accumulated transiently on cortical large endosomes in one-cell-stage embryos as well as in the wild-type embryos, suggesting that the internalization of GFP-CHS-1 is not inhibited in these mutants (Fig. 5B). However, internalized GFP-CHS-1 appeared on the PM again and stably localized to the PM and small vesicles in the mutant embryos (Fig. 5C). This observation suggests that internalized molecules are not efficiently targeted to the lysosomes but recycled to the PM.

We also performed an epistasis test of *ubc-13* or *uev-1* and known endocytic regulators (Fig. 5D). When *rab-5* was knocked down in the *ubc-13(tm3546)* or *uev-1(ok2610)* mutant, GFP-CHS-1 accumulated in small vesicles, as in the wild-type background, suggesting that RAB-5 functions upstream of UBC-13 and UEV-1. Knockdown of *hgrs-1* in wild-type worms resulted in strong accumulation of GFP-CHS-1 in enlarged endosomes. In double mutants of *hgrs-1(RNAi)* and *ubc-13(tm3546)* or *uev-1(ok2610)*, GFP-CHS-1 accumulated on endosomes in the early embryos but appeared on the PM again in the late-stage embryos (Fig. 5D; data not shown). This observation suggests that in *ubc-13* and *uev-1* mutants, cargo molecules are recycled from endosomes to the PM.

### Inhibition of K63-linked ubiquitylation in *ubc-13* and *uev-1* mutants

We examined whether *ubc-13* and *uev-1* mutations affect the ubiquitylation of cargo molecules. The UBC-13/UEV-1 complex is thought to mediate the elongation of K63-linked polyubiquitin chains but not the initiation of ubiquitylation (Ye and Rape, 2009). Because the cytoplasmic region of CAV-1-GFP contains many lysine residues, we expected CAV-1-GFP to accumulate in a multiple monoubiquitylated form in the *ubc-13* or *uev-1* mutant. In *uev-1(ok2610)* and *ubc-13(tm3546)* mutant embryos, CAV-1-GFP accumulated to a level comparable with that observed in *rab-5(RNAi)* embryos, indicating that degradation of CAV-1-GFP was blocked in the mutants (Fig. 3A, lower panel). However, detection of high molecular mass CAV-1-GFP bands by an anti-ubiquitin antibody was lower in *uev-1(ok2610)* and *ubc-13(tm3546)* mutants than in *rab-5(RNAi)* embryos, suggesting that the number of ubiquitin molecules conjugated to CAV-1-GFP was reduced in the mutants (Fig. 3B, top

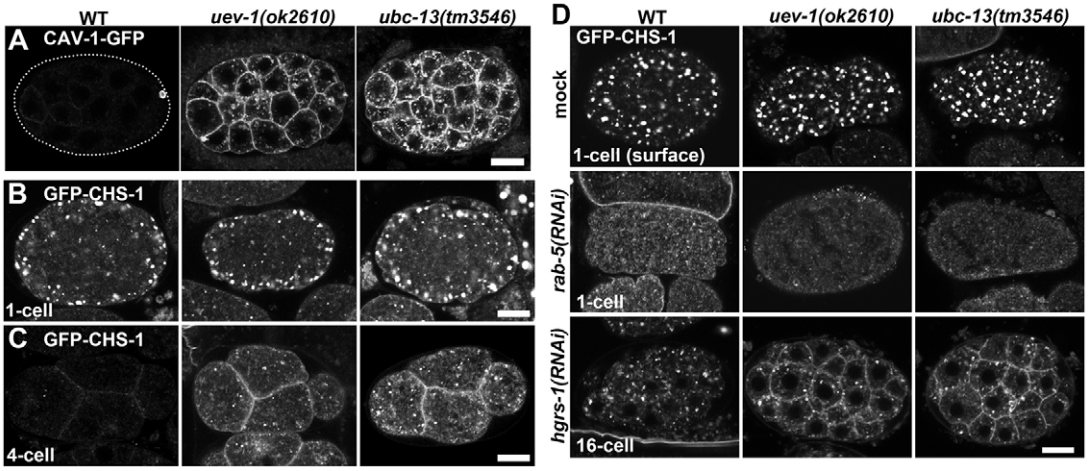


**Fig. 5. UBC-13 and UEV-1 are required for efficient sorting to the MVB pathway.** (A) CAV-1-GFP was expressed in a wild-type, *uev-1(ok2610)* or *ubc-13(tm3546)* background. Images of 16- to 32-cell-stage embryos are shown. (B,C) GFP-CHS-1 was expressed in a wild-type, *uev-1(ok2610)* or *ubc-13(tm3546)* background. Images of one-cell (B) and four-cell (C) stage embryos are shown. (D) RNAi of *rab-5* or *hgrs-1* was performed in a wild-type, *uev-1(ok2610)* or *ubc-13(tm3546)* background, and the subcellular localization of GFP-CHS-1 was examined in embryos. Scale bars: 10 µm.

Development (2014) doi:10.1242/dev.103044

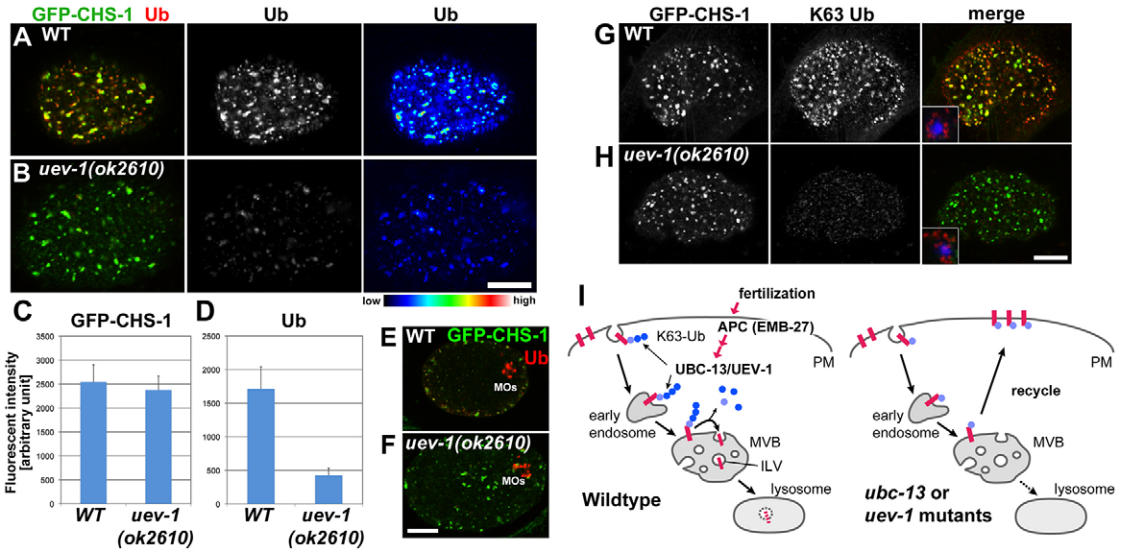


**Fig. 6. UEV-1-dependent accumulation of ubiquitin on endosomes.** (A,B) Embryos dissected from wild-type or *uev-1(ok2610)* animals expressing GFP-CHS-1 were stained with an anti-ubiquitin antibody. Images of one-cell-stage embryos in meiosis II are shown. In the right panels, the fluorescence intensity of the anti-ubiquitin staining is expressed using a pseudocolor scale. (C,D) The fluorescence intensity of GFP-CHS-1 or the anti-ubiquitin staining on endosomes ($n$>120) was quantified in five independent one-cell-stage embryos during meiosis II. (E,F) The middle sections of the same embryos shown in A and B. Merged images of GFP-CHS-1 (green) and ubiquitin (red) are shown. Note that staining of the MOs with an anti-ubiquitin antibody is normal even in the *uev-1(ok2610)* mutant. (G,H) Embryos dissected from wild-type or *uev-1(ok2610)* animals expressing GFP-CHS-1 were stained with an anti-K63-linked ubiquitin antibody. Surface images of one-cell-stage embryos in meiosis II are shown. Insets show MOs in the same embryos. Scale bars: 10 μm. (I) Model of K63-linked polyubiquitin-dependent sorting at the MVB in wild-type embryos (left). In *ubc-13* or *uev-1* mutants, internalized cargo proteins are not efficiently sorted into ILVs, but are recycled to the PM (right).

panel). We also confirmed that the degree of K63-linked ubiquitylation on CAV-1-GFP was greatly reduced in *uev-1(ok2610)* and *ubc-13(tm3546)* mutants (Fig. 3B, second panel). Knockdown of *rab-5* in the *uev-1* mutant enhanced the accumulation of CAV-1-GFP in embryos (Fig. 3A, lower panel). Even under this condition, the total level of ubiquitylation was reduced, and the high molecular mass species of CAV-1-GFP were faintly detected by the anti-K63-linked ubiquitin antibody (Fig. 3B, top and second panels). These results suggest that UBC-13 and UEV-1 regulate the K63-linked ubiquitylation of CAV-1-GFP in embryos. However, we do not exclude the possibility that, in addition to K63-ubiquitin, CAV-1-GFP is modified with other polyubiquitin species, as in the case of endocytic cargo that is modified with mixed polyubiquitin chains of K63 and K11 linkages (Goto et al., 2010). We also assessed total embryonic lysates with immunoblotting (supplementary material Fig. S5E). RNAi of *rab-5* caused proteins modified with K63-linked ubiquitin chains to accumulate, showing that inhibition of endocytic flow results in the bulk accumulation of K63-linked polyubiquitin (supplementary material Fig. S5E). The total reactivity of the anti-K63-linked ubiquitin antibody was reduced in *uev-1(ok2610)* and *ubc-13(tm3546)* mutants, and simultaneous depletion of *uev-1* and *rab-5* prevented the increase in K63-linked ubiquitylation observed with *rab-5* RNAi. Little effect on K48-linked ubiquitin was observed in these strains, although a band of ~200 kDa disappeared as a result of *rab-5* RNAi.

We further examined whether *uev-1* or *ubc-13* mutation affects the transient accumulation of ubiquitin on endosomes (Fig. 6). In the wild-type embryos, the maximum level of anti-ubiquitin staining was observed on cortical endosomes that transiently accumulate endocytic cargo such as GFP-CHS-1 (Fig. 6A). In *uev-1(ok2610)* mutant embryos at this stage, the intensity of anti-ubiquitin staining on endosomes was reduced to ~30% of the staining in wild-type embryos (Fig. 6B). This is consistent with the model in which cargo molecules are (multiply) monoubiquitylated in *ubc-13* or *uev-1* mutants. The intensity of GFP-CHS-1 fluorescence on cortical endosomes was not affected by the *uev-1(ok2610)* mutation, confirming that the internalization of GFP-CHS-1 is almost normal. The anti-K63-linked ubiquitin staining on endosomes was also reduced in *uev-1(ok2610)* mutant embryos, although the staining was not completely abolished (Fig. 6H). Similar results were obtained using *ubc-13(tm3546)* mutant embryos (data not shown). The antibody may weakly react with other polyubiquitin species, and we cannot exclude the possibility that other E2 enzymes are able to mediate K63-linked polyubiquitylation, albeit at a low level. Interestingly, the ubiquitylation of paternal MOs and their subsequent allophagy were not affected in either mutant, showing that this is a UBC-13-independent process (Fig. 6E-H, insets; data not shown).

## DISCUSSION

In this study, we showed that the global ubiquitylation state is dynamically regulated during early development. After fertilization, K63-linked polyubiquitylation is transiently induced, and ubiquitylated proteins accumulate extensively on endosomes. This K63-linked ubiquitylation is required for the efficient sorting of maternal membrane proteins for lysosomal degradation. These results reveal a new physiological function of K63-linked ubiquitylation during the oocyte-to-zygote transition.

The accumulation of K63-linked ubiquitin chains on endosomes is mediated by UBC-13 and UEV-1, the E2 complex that specifically controls K63-linked polyubiquitylation in mammals and yeast. CAV-1-GFP, an endocytic cargo protein, was modified with K63-linked ubiquitin in embryos in a UBC-13-dependent manner. CAV-1-GFP probably accumulates as a multiple monoubiquitylated form in *ubc-13* and *uev-1* mutants. The K63-linked ubiquitylation was first observed on the cell surface in late anaphase I, and the signals further accumulated on endosomes together with cargo proteins in meiosis II. These observations suggest that ubiquitylation begins at the PM level.

Development (2014) doi:10.1242/dev.103044

Consistent with morphological observations, ubiquitylated CAV-1-GFP accumulated in *rab-5(RNAi)* embryos, suggesting that ubiquitylation occurs before proteins reach the early endosomes. Nevertheless, in *ubc-13* and *uev-1* mutant embryos, the internalization of membrane proteins from the PM and their subsequent accumulation on large endosomes appeared almost normal, indicating that K63-linked ubiquitylation is not necessarily essential for internalization from the PM. Instead, the sorting of membrane proteins in the MVB pathway is defective in *ubc-13* and *uev-1* mutants, and cargo molecules are recycled to the PM. These results suggest that K63-linked ubiquitylation is required for sorting into the ILVs rather than for endocytic internalization, which is consistent with studies of yeast Gap1p and the mammalian EGF receptor (Huang et al., 2006; Lauwers et al., 2009). When K63-linked ubiquitylation is impaired by expression of the Ub K63R mutant, internalized Gap1p tends to recycle to the PM (Lauwers et al., 2009). Similarly, endocytosed cargo is recycled from the endosomes to the PM in *ubc-13* and *uev-1* mutants. This phenotype is different from that of *hgrs-1(RNAi)*, in which cargo membrane proteins are stacked in aberrant endosomes. Even in *hgrs-1 ubc-13* double mutants, cargo proteins tend to escape endosomes and recycle to the PM. These results suggest that the ubiquitylation state of cargo proteins (K63-linked ubiquitylation or multiple monoubiquitylation) affects their fate. There may be a mechanism that recognizes and traps proteins modified with K63-linked ubiquitin on endosomes, and this mechanism might be ESCRT-0 independent. Alternatively, monoubiquitylated molecules may actively recycle from the endosomes. Many components of the endocytic machinery are also modified with ubiquitin (Haglund and Dikic, 2012). Although endocytic proteins are monoubiquitylated in most cases, we cannot exclude the possibility that UBC-13 is involved in the ubiquitylation of the endocytic machinery as well as in the ubiquitylation of cargo.

Our results show that degradative endocytic flow is strongly induced after fertilization in *C. elegans*, thus promoting the exchange of cell surface proteins. In mouse embryos, lysosomal number and activity increase after fertilization (Tsukamoto et al., 2013), indicating that this mechanism is conserved in other species. Interestingly, the ubiquitylation and endocytosis of maternal membrane proteins are tightly controlled downstream of the APC. The mechanism that links the meiotic cell cycle and UBC-13-dependent ubiquitylation will be addressed in future studies.

## MATERIALS AND METHODS

### General methods and strains

Methods for the handling and culturing of *C. elegans* were essentially the same as those described previously (Brenner, 1974). The *uev-1(ok2610)* (Kramer et al., 2010) strain was obtained from the *Caenorhabditis* Genetic Center. A deletion allele of *ubc-13(tm3546)* (Kramer et al., 2010) was provided by Shohei Mitani of the Japanese National Bioresource Project for the Experimental Animal 'Nematode *C. elegans*'. In this mutant, a 234-bp region of the *ubc-13* gene is deleted, which creates a stop codon at position C88. Because C88 is the active cysteine essential for E2 activity, the truncated form is thought to lack E2 activity. The original mutant strain was outcrossed with the N2 strain three times. Strains were grown at 20°C, except for *pwIs20* and *pwIs40*, which were grown at 25°C.

RNAi experiments in this study used the feeding method (Kamath et al., 2003). L4 larvae were placed on plates containing nematode growth medium (NGM) agar with 5 mM isopropyl β-D-thiogalactopyranoside and the bacterial strain HT115(DE3) carrying double-stranded RNA expression constructs. The phenotypes were scored after 24 hours or 48 hours (*rab-5* and *hgrs-1*) or in the F1 generation (*ubc-13* and *uev-1*). As a negative control in the RNAi experiments, an L4440 vector harboring the cDNA of human transferrin receptor was used (Sato et al., 2005).

### Plasmids and transgenic *C. elegans*

A genomic fragment containing the coding region of *chs-1* was amplified by polymerase chain reaction (PCR) and cloned into the entry vector pDONR221 using Gateway Recombination Cloning Technology (Invitrogen). *ubq-2* encodes a fusion of ubiquitin and a ribosome L40 subunit. The genomic fragment of *ubq-2* corresponding to the ubiquitin moiety (amino acids 1 to 76) was amplified by PCR and cloned into pDONR221. These fragments were further cloned into the destination vector pID3.01 to express an N-terminal GFP-tagged fusion protein in the oocytes (Pellettieri et al., 2003). A cDNA fragment of *rab-7* was cloned into pDONR201 (Invitrogen) and further transferred into destination vector pKS1, which expresses an N-terminal mRFP fusion under the *pie-1* promoter (Sato et al., 2005). Transgenic lines were created using the microparticle bombardment method as described previously (Praitis et al., 2001). The transgenic lines used in this study were: *dkIs241* [*unc-119(+),* P*pie-1::GFP::chs-1*], *dkIs596* [*unc-119(+),* P*pie-1::GFP::ubq-2*] and *pwIs40* [*unc-119(+),* P*pie-1::mRFP::rab-7*] (this study); *pwIs281* [*unc-119(+),* P*pie-1::cav-1::GFP*] (Sato et al., 2006); *pwIs20* [*unc-119(+),* P*pie-1::GFP::rab-5*] (Sato et al., 2005); *bIs1* [*vit-2::GFP*] (Grant and Hirsh, 1999); *pwIs116* [*unc-119(+),* P*pie-1::rme-2::GFP*] (Balklava et al., 2007); *pwIs21* [*unc-119(+),* P*pie-1::GFP::rab-7*] (Sato and Sato, 2011); and *teIs1* [*unc-119(+), oma-1::GFP*] (Lin, 2003).

cDNAs of *ubc-13* and *rab-5* were subcloned into pDONR221 and further into L4440 using Gateway Recombination Cloning Technology for RNAi experiments. RNAi of *uev-1* or *hgrs-1* was performed using plasmids recovered from the genome-wide RNAi library (Kamath et al., 2003).

### Microscopy and immunostaining

To observe live worms expressing transgenes, worms were mounted on agarose pads with 20 mM levamisole in M9 buffer. Dissected embryos were permeabilized and fixed by a freeze-crack method (Sato and Sato, 2011). Embryos were fixed sequentially in methanol at –20°C for 5 minutes and in acetone at –20°C for 2 minutes. Fixed embryos were then blocked with PTB (PBS containing 1% BSA, 0.1% Tween 20, 0.05% $NaN_3$ and 1 mM EDTA) and stained with anti-ubiquitin antibodies or an anti-RME-2 antibody (Grant and Hirsh, 1999). An anti-polyubiquitin (FK2) antibody was purchased from Medical and Biological Laboratories (Nagoya, Japan). Anti-polyubiquitin antibodies specific for K48 and K63 linkages (Apu2 and Apu3, respectively) were purchased from Millipore. An anti-K63-linked polyubiquitin antibody (D7A11) was purchased from Cell Signaling Technology Japan. For pre-absorption, Apu2 and Apu3 antibodies were preincubated for 1 hour at room temperature with a 10-fold excess of purified K48-linked penta-ubiquitin or K63-linked tetra-ubiquitin (Boston Biochem). Confocal images were obtained using an Olympus FV1000 confocal microscope system equipped with a 60×, 1.35 NA UPlanSApo oil-objective lens (Olympus). Fluorescent signals were quantified using MetaMorph software (Molecular Devices).

### Immunoblotting and immunoprecipitation

Total worm lysates were prepared from 40 adult hermaphrodites as described previously (Sato et al., 2005) and assessed by immunoblotting using a goat anti-GFP polyclonal antibody (Fitzgerald Industries International) or an anti-actin antibody (C4; Millipore). Embryos were collected from gravid adult worms by a bleaching method (Stiernagle, 1999), and embryos washed with M9 buffer were resuspended in a small amount of M9 buffer. An equal amount of 2× lysis buffer [125 mM Tris-HCl, pH 6.8, 6% SDS, 20% glycerol, 2 mM phenylmethylsulfonyl fluoride (PMSF)] was added to each embryo suspension. The suspensions were immediately frozen at −20°C and then incubated at 60°C for 25 minutes. Lysates were cleared by centrifugation at 16,200 ***g*** for 10 minutes. The embryonic lysates (70 μg) were diluted with 30 volumes of IP buffer (50 mM Tris-HCl, pH 7.4, 150 mM NaCl, 5 mM EDTA, 1% Triton X-100, 1 mM PMSF) and incubated with a goat anti-GFP polyclonal antibody (Fitzgerald Industries) at 4°C overnight and then incubated with protein-G-Sepharose (Sigma-Aldrich) for 4 hour at 4°C. Beads were washed with IP buffer five times, and IP buffer without Triton X-100 once. Precipitates were eluted with Laemmli sampling buffer and immunoblotted using an anti-ubiquitin (P4D1; Santa Cruz Biotechnology), anti-K63-linked ubiquitin

(Apu3), anti-K48-linked ubiquitin (Apu2) or anti-GFP polyclonal (Medical and Biological Laboratories) antibody.

**Acknowledgements**
We thank members of Ken Sato's laboratory, N. Matsuda, F. Tokunaga and B. D. Grant, for their technical assistance and discussions; and S. Mitani and the Caenorhabditis Genetic Center for supplying strains.

**Competing interests**
The authors declare no competing financial interests.

**Author contributions**
M.S. and Ken Sato designed experiments, analyzed data and wrote the manuscript. M.S., R.K., Katsuya Sato and K.T. performed experiments.

**Funding**
This research was supported by a Grant-in-Aid for Young Scientists (A) from the Japan Society for the Promotion of Science [23687027 to M.S.]; a Grant-in-Aid for Scientific Research on Innovative Areas from the Ministry of Education, Culture, Sports, Science and Technology [23113703 to M.S.]; the Naito Foundation (M.S. and Ken Sato); the Cell Science Research Foundation (M.S.); and a Shiseido Female Researcher Science Grant (M.S.). This research was also supported by the Funding Program for Next Generation World-leading Researchers (NEXT program), the Sumitomo Foundation, and the Mochida Memorial Foundation (Ken Sato).

**Supplementary material**
Supplementary material available online at
http://dev.biologists.org/lookup/suppl/doi:10.1242/dev.103044/-/DC1

**References**

**Al Rawi, S., Louvet-Vallée, S., Djeddi, A., Sachse, M., Culetto, E., Hajjar, C., Boyd, L., Legouis, R. and Galy, V.** (2011). Postfertilization autophagy of sperm organelles prevents paternal mitochondrial DNA transmission. *Science* **334**, 1144-1147.
**Audhya, A., McLeod, I. X., Yates, J. R. and Oegema, K.** (2007). MVB-12, a fourth subunit of metazoan ESCRT-I, functions in receptor downregulation. *PLoS ONE* **2**, e956.
**Balklava, Z., Pant, S., Fares, H. and Grant, B. D.** (2007). Genome-wide analysis identifies a general requirement for polarity proteins in endocytic traffic. *Nat. Cell Biol.* **9**, 1066-1073.
**Barriere, H., Nemes, C., Du, K. and Lukacs, G. L.** (2007). Plasticity of polyubiquitin recognition as lysosomal targeting signals by the endosomal sorting machinery. *Mol. Biol. Cell* **18**, 3952-3965.
**Bowerman, B. and Kurz, T.** (2006). Degrade to create: developmental requirements for ubiquitin-mediated proteolysis during early C. elegans embryogenesis. *Development* **133**, 773-784.
**Brenner, S.** (1974). The genetics of Caenorhabditis elegans. *Genetics* **77**, 71-94.
**Deng, L., Wang, C., Spencer, E., Yang, L., Braun, A., You, J., Slaughter, C., Pickart, C. and Chen, Z. J.** (2000). Activation of the IkappaB kinase complex by TRAF6 requires a dimeric ubiquitin-conjugating enzyme complex and a unique polyubiquitin chain. *Cell* **103**, 351-361.
**Eddins, M. J., Carlile, C. M., Gomez, K. M., Pickart, C. M. and Wolberger, C.** (2006). Mms2-Ubc13 covalently bound to ubiquitin reveals the structural basis of linkage-specific polyubiquitin chain formation. *Nat. Struct. Mol. Biol.* **13**, 915-920.
**Erpapazoglou, Z., Dhaoui, M., Pantazopoulou, M., Giordano, F., Mari, M., Léon, S., Raposo, G., Reggiori, F. and Haguenauer-Tsapis, R.** (2012). A dual role for K63-linked ubiquitin chains in multivesicular body biogenesis and cargo sorting. *Mol. Biol. Cell* **23**, 2170-2183.
**Fukushima, T., Matsuzawa, S., Kress, C. L., Bruey, J. M., Krajewska, M., Lefebvre, S., Zapata, J. M., Ronai, Z. and Reed, J. C.** (2007). Ubiquitin-conjugating enzyme Ubc13 is a critical component of TNF receptor-associated factor (TRAF)-mediated inflammatory responses. *Proc. Natl. Acad. Sci. USA* **104**, 6371-6376.
**Goto, E., Yamanaka, Y., Ishikawa, A., Aoki-Kawasumi, M., Mito-Yoshida, M., Ohmura-Hoshino, M., Matsuki, Y., Kajikawa, M., Hirano, H. and Ishido, S.** (2010). Contribution of lysine 11-linked ubiquitination to MIR2-mediated major histocompatibility complex class I internalization. *J. Biol. Chem.* **285**, 35311-35319.
**Grant, B. and Hirsh, D.** (1999). Receptor-mediated endocytosis in the Caenorhabditis elegans oocyte. *Mol. Biol. Cell* **10**, 4311-4326.
**Haglund, K. and Dikic, I.** (2012). The role of ubiquitylation in receptor endocytosis and endosomal sorting. *J. Cell Sci.* **125**, 265-275.
**Hofmann, R. M. and Pickart, C. M.** (1999). Noncanonical MMS2-encoded ubiquitin-conjugating enzyme functions in assembly of novel polyubiquitin chains for DNA repair. *Cell* **96**, 645-653.
**Huang, F., Kirkpatrick, D., Jiang, X., Gygi, S. and Sorkin, A.** (2006). Differential regulation of EGF receptor internalization and degradation by multiubiquitination within the kinase domain. *Mol. Cell* **21**, 737-748.
**Johnston, W. L. and Dennis, J. W.** (2012). The eggshell in the C. elegans oocyte-to-embryo transition. *Genesis* **50**, 333-349.
**Johnston, W. L., Krizus, A. and Dennis, J. W.** (2010). Eggshell chitin and chitin-interacting proteins prevent polyspermy in C. elegans. *Curr. Biol.* **20**, 1932-1937.
**Kadandale, P., Stewart-Michaelis, A., Gordon, S., Rubin, J., Klancer, R., Schweinsberg, P., Grant, B. D. and Singson, A.** (2005). The egg surface LDL receptor repeat-containing proteins EGG-1 and EGG-2 are required for fertilization in Caenorhabditis elegans. *Curr. Biol.* **15**, 2222-2229.
**Kamath, R. S., Fraser, A. G., Dong, Y., Poulin, G., Durbin, R., Gotta, M., Kanapin, A., Le Bot, N., Moreno, S., Sohrmann, M. et al.** (2003). Systematic functional analysis of the Caenorhabditis elegans genome using RNAi. *Nature* **421**, 231-237.
**Kerscher, O., Felberbaum, R. and Hochstrasser, M.** (2006). Modification of proteins by ubiquitin and ubiquitin-like proteins. *Annu. Rev. Cell Dev. Biol.* **22**, 159-180.
**Kramer, L. B., Shim, J., Previtera, M. L., Isack, N. R., Lee, M. C., Firestein, B. L. and Rongo, C.** (2010). UEV-1 is an ubiquitin-conjugating enzyme variant that regulates glutamate receptor trafficking in C. elegans neurons. *PLoS ONE* **5**, e14291.
**L'Hernault, S. W.** (2006). Spermatogenesis. In *WormBook* (ed. The C. elegans Research Community). doi/10.1895/wormbook.1.85.1, http://www.wormbook.org.
**Lauwers, E., Jacob, C. and André, B.** (2009). K63-linked ubiquitin chains as a specific signal for protein sorting into the multivesicular body pathway. *J. Cell Biol.* **185**, 493-502.
**Lauwers, E., Erpapazoglou, Z., Haguenauer-Tsapis, R. and André, B.** (2010). The ubiquitin code of yeast permease trafficking. *Trends Cell Biol.* **20**, 196-204.
**Lin, R.** (2003). A gain-of-function mutation in oma-1, a C. elegans gene required for oocyte maturation, results in delayed degradation of maternal proteins and embryonic lethality. *Dev. Biol.* **258**, 226-239.
**Maruyama, R., Velarde, N. V., Klancer, R., Gordon, S., Kadandale, P., Parry, J. M., Hang, J. S., Rubin, J., Stewart-Michaelis, A., Schweinsberg, P. et al.** (2007). EGG-3 regulates cell-surface and cortex rearrangements during egg activation in Caenorhabditis elegans. *Curr. Biol.* **17**, 1555-1560.
**Mayers, J. R., Wang, L., Pramanik, J., Johnson, A., Sarkeshik, A., Wang, Y., Saengsawang, W., Yates, J. R., III and Audhya, A.** (2013). Regulation of ubiquitin-dependent cargo sorting by multiple endocytic adaptors at the plasma membrane. *Proc. Natl. Acad. Sci. USA* **110**, 11857-11862.
**McCarter, J., Bartlett, B., Dang, T. and Schedl, T.** (1999). On the control of oocyte meiotic maturation and ovulation in Caenorhabditis elegans. *Dev. Biol.* **205**, 111-128.
**Mukhopadhyay, D. and Riezman, H.** (2007). Proteasome-independent functions of ubiquitin in endocytosis and signaling. *Science* **315**, 201-205.
**Newton, K., Matsumoto, M. L., Wertz, I. E., Kirkpatrick, D. S., Lill, J. R., Tan, J., Dugger, D., Gordon, N., Sidhu, S. S., Fellouse, F. A. et al.** (2008). Ubiquitin chain editing revealed by polyubiquitin linkage-specific antibodies. *Cell* **134**, 668-678.
**Pellettieri, J., Reinke, V., Kim, S. K. and Seydoux, G.** (2003). Coordinate activation of maternal protein degradation during the egg-to-embryo transition in C. elegans. *Dev. Cell* **5**, 451-462.
**Pickart, C. M. and Fushman, D.** (2004). Polyubiquitin chains: polymeric protein signals. *Curr. Opin. Chem. Biol.* **8**, 610-616.
**Praitis, V., Casey, E., Collar, D. and Austin, J.** (2001). Creation of low-copy integrated transgenic lines in Caenorhabditis elegans. *Genetics* **157**, 1217-1226.
**Raiborg, C. and Stenmark, H.** (2009). The ESCRT machinery in endosomal sorting of ubiquitylated membrane proteins. *Nature* **458**, 445-452.
**Sato, M. and Sato, K.** (2011). Degradation of paternal mitochondria by fertilization-triggered autophagy in C. elegans embryos. *Science* **334**, 1141-1144.
**Sato, M. and Sato, K.** (2013). Dynamic regulation of autophagy and endocytosis for cell remodeling during early development. *Traffic* **14**, 479-486.
**Sato, M., Sato, K., Fonarev, P., Huang, C. J., Liou, W. and Grant, B. D.** (2005). Caenorhabditis elegans RME-6 is a novel regulator of RAB-5 at the clathrin-coated pit. *Nat. Cell Biol.* **7**, 559-569.
**Sato, K., Sato, M., Audhya, A., Oegema, K., Schweinsberg, P. and Grant, B. D.** (2006). Dynamic regulation of caveolin-1 trafficking in the germ line and embryo of Caenorhabditis elegans. *Mol. Biol. Cell* **17**, 3085-3094.
**Sato, M., Grant, B. D., Harada, A. and Sato, K.** (2008). Rab11 is required for synchronous secretion of chondroitin proteoglycans after fertilization in Caenorhabditis elegans. *J. Cell Sci.* **121**, 3177-3186.
**Spike, C. A. and Strome, S.** (2003). Germ plasm: protein degradation in the soma. *Curr. Biol.* **13**, R837-R839.
**Stiernagle, T.** (1999). Maintenance of C. elegans. In *C. elegans; A Practical Approach* (ed. I. A. Hope), pp. 51-67. Oxford: Oxford University Press.
**Stitzel, M. L. and Seydoux, G.** (2007). Regulation of the oocyte-to-zygote transition. *Science* **316**, 407-408.
**Stitzel, M. L., Cheng, K. C. and Seydoux, G.** (2007). Regulation of MBK-2/Dyrk kinase by dynamic cortical anchoring during the oocyte-to-zygote transition. *Curr. Biol.* **17**, 1545-1554.
**Stringer, D. K. and Piper, R. C.** (2011). A single ubiquitin is sufficient for cargo protein entry into MVBs in the absence of ESCRT ubiquitination. *J. Cell Biol.* **192**, 229-242.
**Traub, L. M. and Lukacs, G. L.** (2007). Decoding ubiquitin sorting signals for clathrin-dependent endocytosis by CLASPs. *J. Cell Sci.* **120**, 543-553.
**Tsukamoto, S., Hara, T., Yamamoto, A., Ohta, Y., Wada, A., Ishida, Y., Kito, S., Nishikawa, T., Minami, N., Sato, K. et al.** (2013). Functional analysis of lysosomes during mouse preimplantation embryo development. *J. Reprod. Dev.* **59**, 33-39.
**Wu, X., Yamamoto, M., Akira, S. and Sun, S. C.** (2009). Regulation of hematopoiesis by the K63-specific ubiquitin-conjugating enzyme Ubc13. *Proc. Natl. Acad. Sci. USA* **106**, 20836-20841.
**Yamamoto, M., Okamoto, T., Takeda, K., Sato, S., Sanjo, H., Uematsu, S., Saitoh, T., Yamamoto, N., Sakurai, H., Ishii, K. J. et al.** (2006). Key function for the Ubc13 E2 ubiquitin-conjugating enzyme in immune receptor signaling. *Nat. Immunol.* **7**, 962-970.
**Ye, Y. and Rape, M.** (2009). Building ubiquitin chains: E2 enzymes at work. *Nat. Rev. Mol. Cell Biol.* **10**, 755-764.

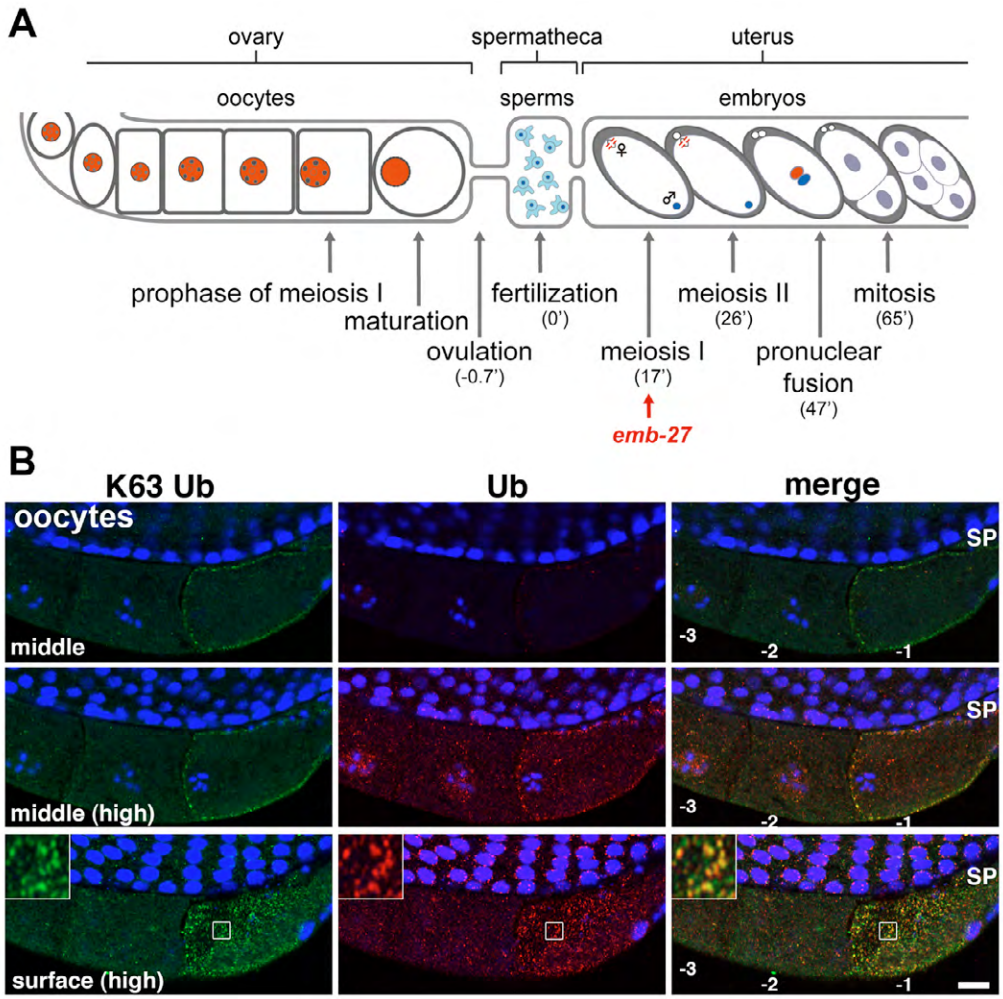


**Figure S1. Relatively weak ubiquitin staining is observed in oocytes.**
(A) Stylized drawing of one gonad arm connected to the spermatheca and the uterus. The landmark events before and after fertilization and their typical time course are indicated. In *C. elegans*, oocytes of the hermaphrodite gonad are arrested in diakinesis of meiotic prophase I. The mature oocyte ovulates and enters the spermatheca containing sperms, which is followed by immediate fertilization (1 oocyte ovulates every 23 min, on average). After fertilization, embryos move to the uterus, complete meiosis I and meiosis II, and start zygotic development. *emb-27(RNAi)* blocks the metaphase to anaphase transition of meiosis I. (B) The wild-type N2 gonads were dissected from adult hermaphrodites and stained with an anti-ubiquitin antibody (red), an anti-K63-linked ubiquitin antibody (green), and DAPI (blue). The upper images were acquired under the same condition used in Fig. 1 A–C. Images of the same oocytes were also obtained using a higher laser power (middle and lower panels). Embryos are numbered by the position from the spermatheca. SP, spermatheca. Enlarged images (×4) are shown as insets. Bar, 10 μm.

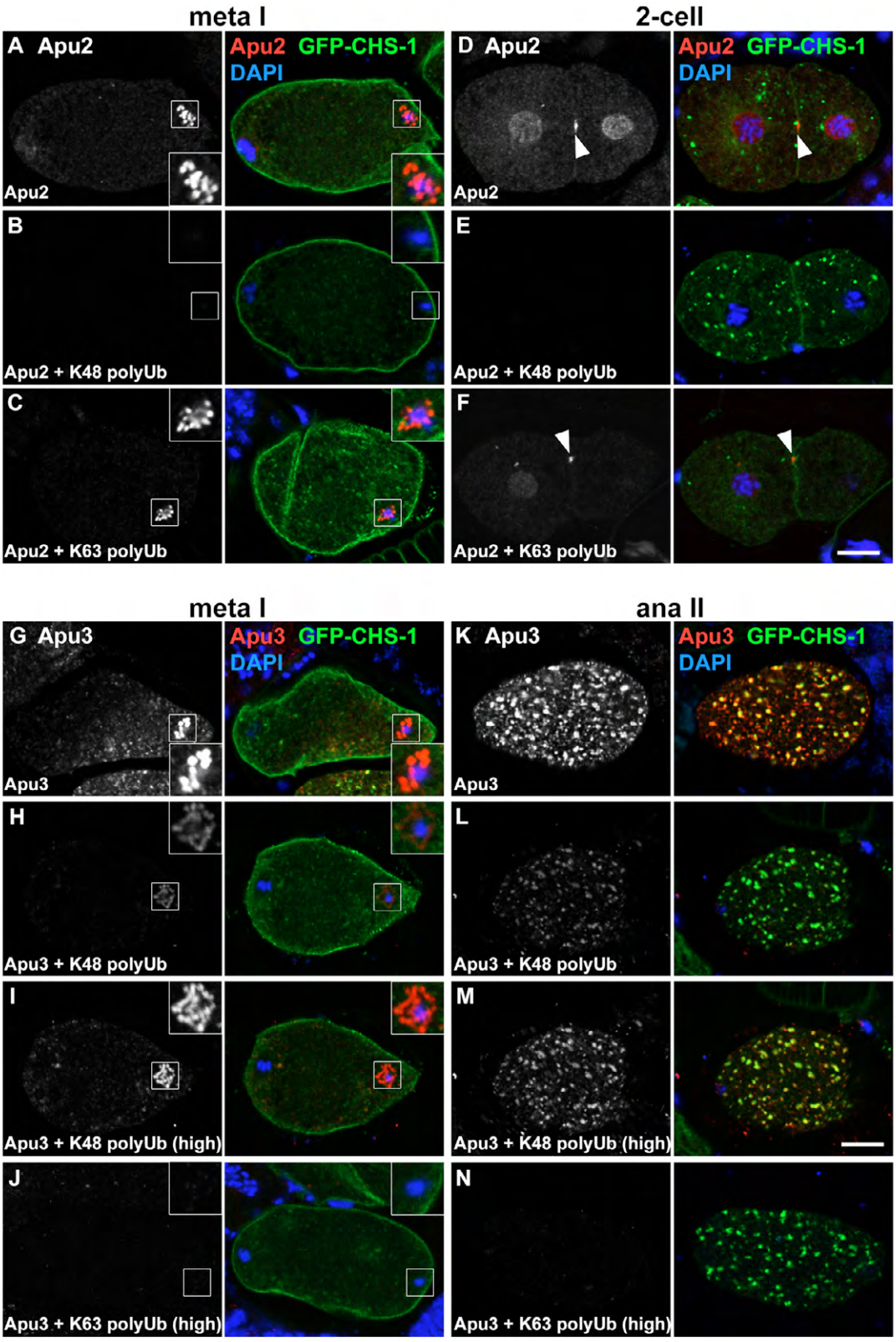


**Figure S2. Specificity of anti-K48-ubiquitin and anti-K63-linked ubiquitin antibodies.**
(A-F) Embryos expressing GFP-CHS-1 were stained with the anti-K48-linked ubiquitin antibody (Apu2) or the antibody preincubated with purified K48- or K63-linked polyubiquitin. Embryos in metaphase I (A–C) and the 2-cell stage (J–N) are shown. Insets show the MO staining (×2), and arrowheads in F indicate the cleavage furrow. All images were acquired under the same conditions. (G-N) Embryos expressing GFP-CHS-1 were stained with the anti-K63-linked ubiquitin antibody (Apu3) or the antibody preincubated with purified K48- or K63-linked polyubiquitin. Embryos in metaphase I (G–J) and anaphase II (K–N) are shown. Images in I, J, M, and N were acquired using a higher laser power. Insets show the MO staining (×2). Merged images of antibody staining, GFP-CHS-1, and DAPI are shown for reference. Bar, 10 μm.

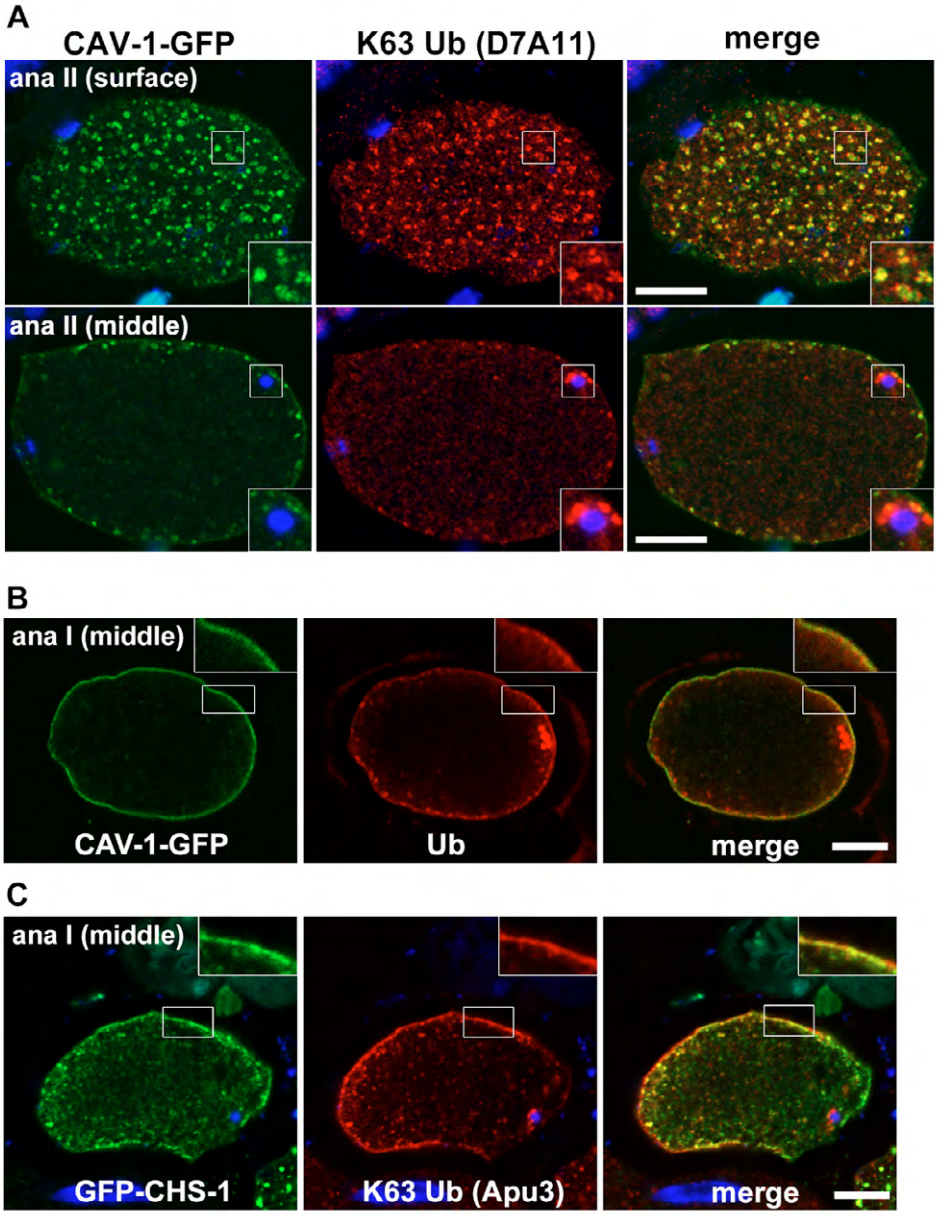


**Figure S3. Ubiquitination is detectable on the PM in late anaphase I.**
(A) Embryos expressing CAV-1-GFP were stained with an anti-K63-linked ubiquitin antibody (D7A11). Surface and middle sections of an embryo in anaphase II are shown. Insets (×2) show endosomes (upper panel) and the MOs (lower panel). (B and C) Embryos expressing CAV-1-GFP or GFP-CHS-1 were stained with an anti-ubiquitin antibody (FK2; B) or an anti-K63-linked ubiquitin antibody (Apu3; C), respectively. Embryos in late anaphase I are shown. Ubiquitin staining was detected on the PM in this stage. Insets show enlarged images of the boxed area. Bars, 10 μm.

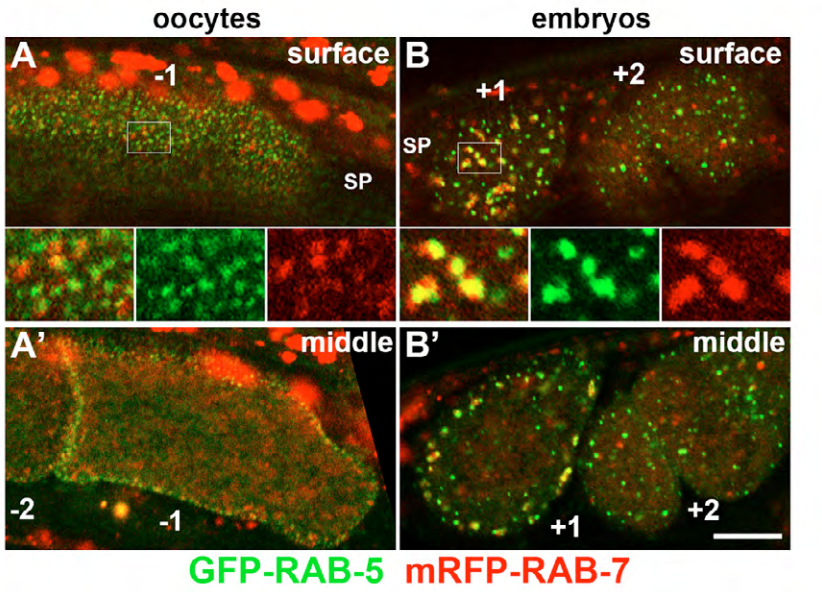


**Figure S4. RAB-5- and RAB-7-positive endosomes are remodeled after fertilization.**
Subcellular localization of GFP-RAB-5 (green) and mRFP-RAB-7 (red) in oocytes and embryos of a single hermaphrodite. The surface (A and B) and middle (A' and B') planes of oocytes (A and A') and embryos (B and B') are shown. All images were acquired under the same conditions. In A and B, enlarged images (×3) of the boxed areas are also shown. SP, spermatheca. Bar, 10 μm.

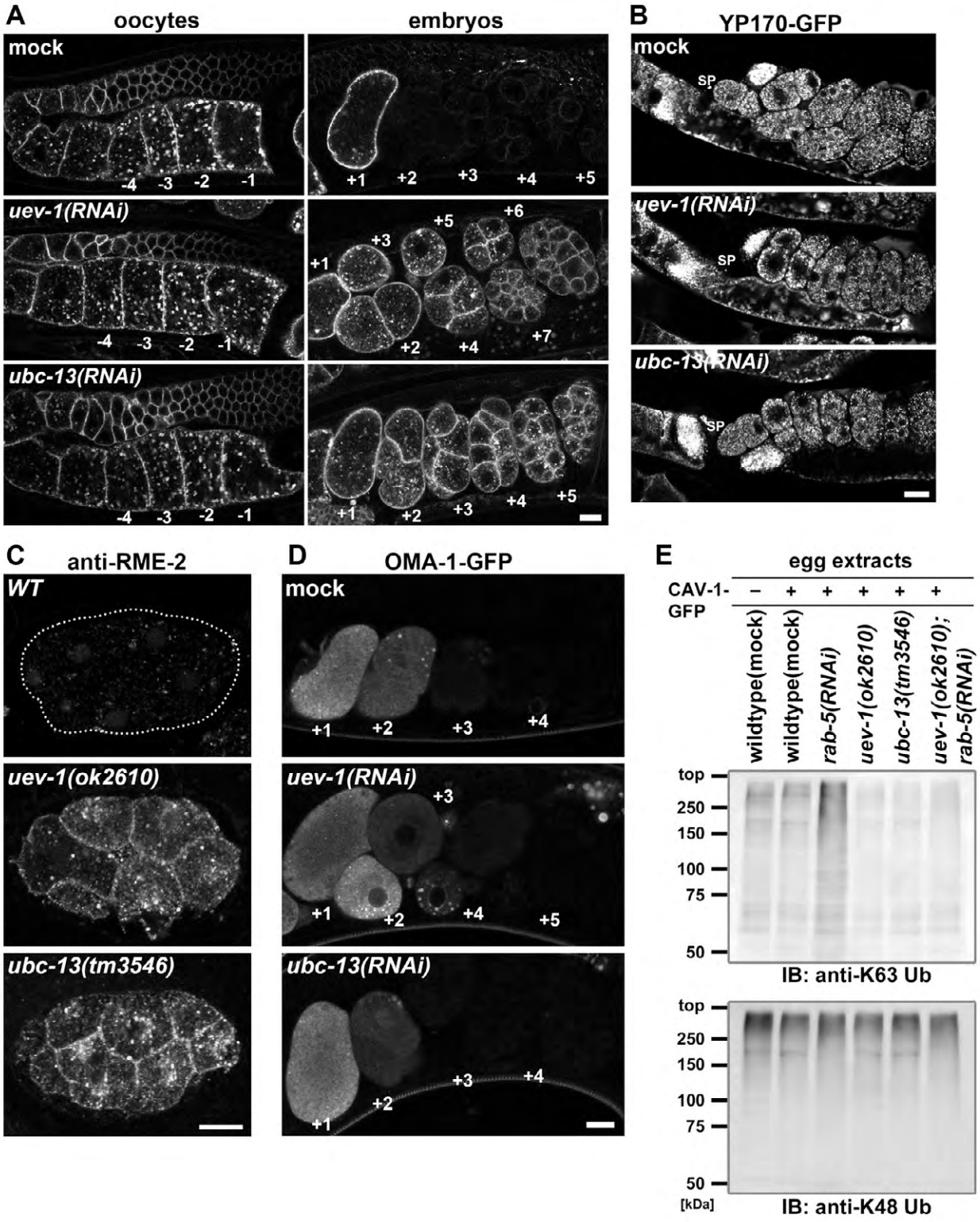


**Figure S5. Phenotypes of *ubc-13* and *uev-1* mutants.**
(A) RNAi of *ubc-13* or *uev-1* inhibits clearance of CAV-1-GFP in embryos. Oocytes and embryos were observed in wild-type worms and in *ubc-13(RNAi)* or *uev-1(RNAi)* mutants expressing CAV-1-GFP. (B) Yolk uptake was normal in *ubc-13* and *uev-1* mutants. Worms expressing VIT-2-GFP were treated with *ubc-13* or *uev-1* RNAi. (C) Degradation of endogenous RME-2 was inhibited in *ubc-13* and *uev-1* mutants. Wild-type embryos and *ubc-13(tm3546)* or *uev-1(ok2610)* mutant embryos were stained with an anti-RME-2 antibody. The 8-cell stage embryos are shown. (D) Degradation of OMA-1-GFP was normal in *ubc-13* and *uev-1* mutants. Worms expressing OMA-1-GFP were treated with *ubc-13* or *uev-1* RNAi. Embryos are numbered by the position from the spermatheca. Bars, 10 μm. (E) Embryo lysates (10 μg) were prepared from the indicated strains and probed with anti-K63- and anti-K48-linked ubiquitin antibodies.